

Microstructural changes to metal bond coatings on gas turbine alloys with time at high temperature

N. V. RUSSELL, F. WIGLEY, J. WILLIAMSON

Department of Materials, Imperial College, Prince Consort Road, London SW7 2BP, UK
E-mail: n.russell@ic.ac.uk

Complex coating systems are required to protect nickel-based superalloys from high temperature oxidation and corrosion. Industrial gas turbine blades and heat shields are generally plasma sprayed with a metal bond coating containing nickel, chromium, cobalt, aluminium and yttrium, and then an external thermal barrier coating of yttria-stabilised zirconia is applied. In this study, samples of an IN939 alloy heat shield with both a metal bond coat and a ceramic thermal barrier coating have been heated in air at high temperature for up to 2000 hours to assess the long term stability of the metal bond coat. Polished sections of the heat treated samples were examined by SEM and EDX to determine microstructural changes. The Ni-Cr-Co-Al-Y coating was found to be a very effective barrier against oxidation; the only apparent oxidation being the growth of an alumina layer between the bond coat and ceramic thermal barrier coating. With time, the growth of the γ' Ni₃Al phase in the metallic bond coat was observed, with extensive diffusion of other elements to and from the bond coat. © 2000 Kluwer Academic Publishers

1. Introduction

Complex coating systems are required to protect nickel-based superalloys from high temperature oxidation and corrosion. Industrial gas turbine blades and heat shields are generally plasma sprayed with a metal bond coat (~250 μm thick) containing nickel, chromium, cobalt, aluminium and yttrium, then an external thermal barrier coating (~500 μm) of yttria-stabilised zirconia is applied. The bond coat provides oxidation/corrosion protection to the underlying superalloy, while the outer thermal barrier coating lowers the metal temperatures to reduce rates of oxidation and extend service life. Oxidation of the metal bond coat eventually leads to degradation and blistering of the thermal barrier coating. Coatings may be refurbished; the life expectancy of components in industrial gas turbines is currently in excess of 50,000 hours [1].

The functions and properties of the coatings [1–7] have been summarised in Table I. Coating failure is influenced by bond coat oxidation, but the failure occurs in the oxygen-transparent ceramic coating [4]. Thermal stresses between coatings bring about the failure of the thermal barrier by ceramic layer spallation [3]. Spalling can be reduced by controlling the coating structure, e.g. by introducing cracks into the layer, so that local stresses are minimised.

The metal bond coat provides protection from the environment to the underlying superalloy by forming a thin surface oxide scale. Under oxidising conditions, an alumina (Al₂O₃) scale forms at ~870°C and is stable to ~1200°C [3]. Although the alumina scale spalls during

thermal cycling, the bond coat acts as a reservoir of aluminium so that rapid repair of the surface oxide can occur [1, 8]. This process continues until the outward flux of aluminium is insufficient to form a continuous protective scale, bringing on rapid degradation of the underlying bond coat and base superalloy.

In this study, samples of IN939 superalloy combustion chamber heat shield with both a metal bond coat and ceramic thermal barrier coating have been heat treated in air at high temperature for up to 2000 hours to assess the long term stability of the metal bond coat. Under normal operating conditions, the temperature at the bond coat surface is ~950°C, however, excursions to 1050°C may be experienced. 1075°C was chosen for the laboratory study to assess the oxidation and diffusion processes and changes to the coating microstructure over a reasonable timescale.

2. Experimental details

The heat shield had been in service for ~1000 hours and, under normal conditions, would have seen temperatures of ~1250°C at the front face, ~950°C at the metal bond coat surface and ~500°C at the air-cooled back of the base superalloy. The metal bond coat and thermal barrier coating had both been plasma sprayed on to the base superalloy. Plasma sprayed coatings have been demonstrated to provide excellent oxidation resistance and moderate thermal fatigue resistance, with Ni-Cr-Co-Al-Y coatings having a lifetime five times longer than nickel aluminide coatings [7]. The samples

TABLE I Function and properties of coating systems [1–7]

Bond coat properties	Thermal barrier coating function
<ul style="list-style-type: none"> • High oxidation resistance • Compatibility with base alloy • Low rate of interdiffusion between the coating and alloy • Ductility to withstand dimensional changes between the alloy and ceramic coating without cracking • High strength at elevated temperatures 	<ul style="list-style-type: none"> • Lowers superalloy temperature to prolong lifetime • Reduced amount of thermally-induced strain in the bond coat and superalloy • Reduced volume of cooling air required thereby increasing turbine efficiency

were heat treated in air (at a flow rate of 200 mlmin⁻¹) in a controlled atmosphere furnace at 1075°C for periods of 300, 600, 900, 1200, 1500 and 2000 hours without thermal cycling. A sample was retained unheated.

Following heat treatment, one piece from each heat treatment time was set in resin and the surface ground to 6 μm using silicon carbide papers. The samples were then polished with diamond to a 0.25 μm finish. The samples were carbon coated prior to SEM examination.

The microstructures were examined in a JEOL JSM-6400 SEM. An accelerating voltage of 20 kV was used to excite the M-lines of elements such as Ta and W. Elemental analyses were carried out by energy dispersive X-ray spectroscopy (EDX). Quantitative chemical and image analysis data was acquired using a NORAN light element detector and Voyager 4 software.

3. Results and discussion

Fig. 1a shows a low magnification back-scattered electron image of a section through the untreated, “as received”, sample. The heat shield consists of base metal

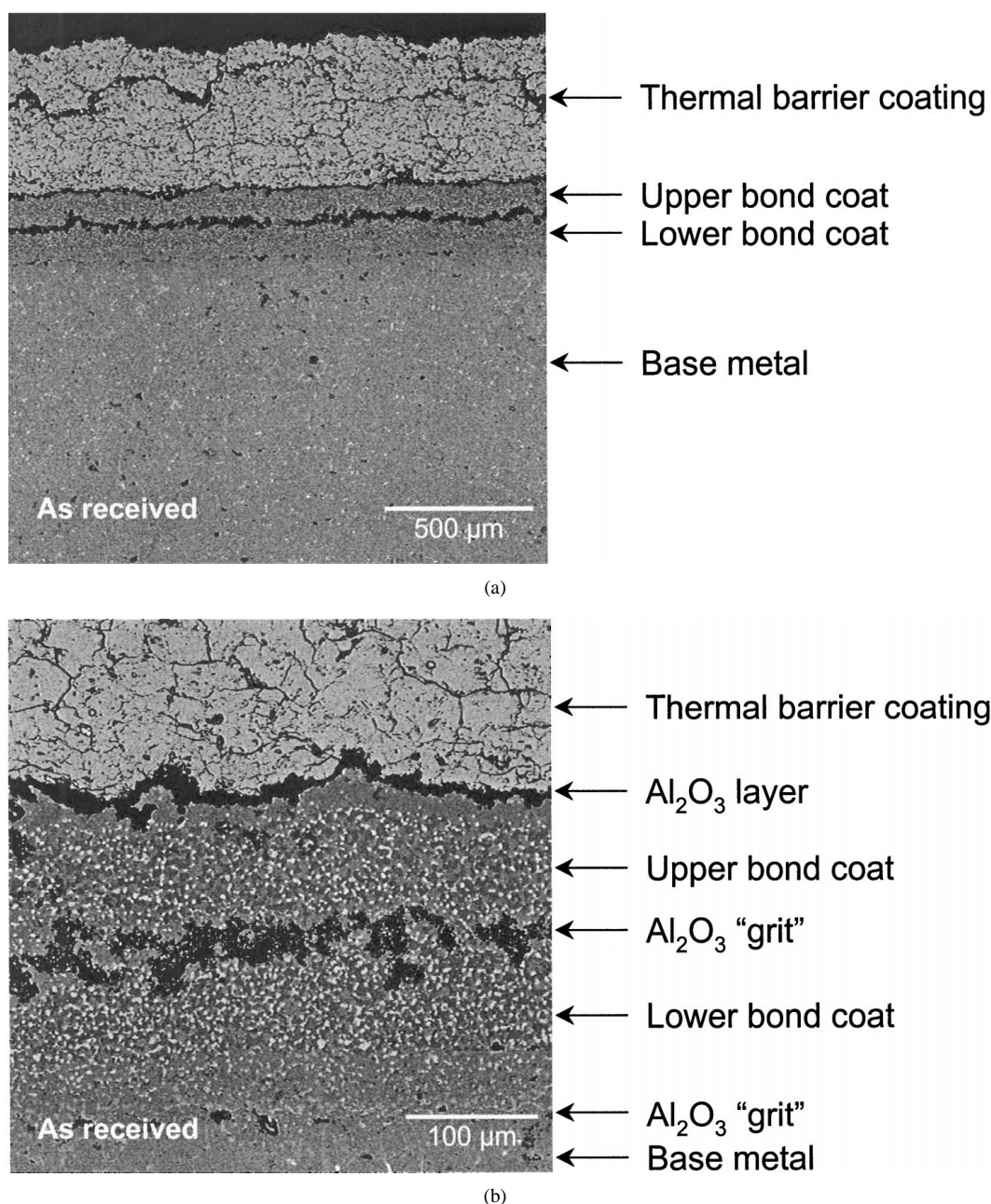


Figure 1 (a) Back-scattered electron image overview of the untreated sample, showing the thickness of the thermal barrier coating and bond coat. (b) Detail of the bond coat region showing the complex multi-phase microstructure.

TABLE II Chemical analyses of “as received” sample (in wt%)

Element	Base metal (IN939)	Lower bond coat	Upper bond coat	Thermal barrier coating
Oxygen	—	—	—	12.6
Aluminium	1.9	12.5	12.9	—
Titanium	4.2	1.0	—	—
Chromium	22.7	18.9	18.9	—
Cobalt	17.9	11.0	10.6	—
Nickel	47.0	53.0	53.0	—
Yttrium	—	1.2	0.6	7.1
Zirconium	—	—	—	76.0
Hafnium	—	—	—	2.5

Small quantities of other elements provide the balance of 100 wt%

protected by a bond coat and a thermal barrier coating. The pre-cracked thermal barrier coating is approximately 500 μm thick. The bond coat consists of two layers, termed here “upper” and “lower”, and is approximately 250 μm thick. The composition of the upper bond coat may be optimised for corrosion resistance, whereas the lower coating may provide good adhesion and metallurgical stability at the coating/base superalloy interface [9]. Fig. 1b shows the multi-phased bond coat region in more detail. The bulk chemical analyses of the heat shield and coatings are displayed in Table II. The base metal is IN939. Both the lower and upper bond coats are Ni-Cr-Co-Al-Y based. The thermal barrier coating is an yttria-stabilised zirconia (8 wt% Y_2O_3) ceramic. There is an alumina (Al_2O_3) layer, about 15 μm thick (Fig. 1b) between the thermal barrier coating and the upper bond coat. A layer of alumina “grit” separates the upper and lower bond coats, and the lower bond coat from the base metal. It has been shown that this grit improves the mechanical bond and moves the failure location away from the interface to within the bond coat [10].

Both the upper and lower bond coats contain four phases, Table III. These phases have been designated by their intensities in the back-scattered electron image. The white-coloured phase in both is rich in chromium. In the lower bond coat, the black-coloured phase is rich in titanium and also contains nitrogen. The light-grey phase is rich in nickel and aluminium, the dark-grey phase is similar but also contains a small amount of yttrium. In the upper bond coat, the black-coloured phase is rich in aluminium and also contains nitrogen.

TABLE III Chemical analyses (in wt%) of the phases present in the lower and upper bond coat of the “as received” sample

Phases	Al	Ti	Cr	Co	Ni	Y	N	Others*
<u>LBC</u> area	12.5	1.0	18.9	11.0	53.0	1.2	—	2.4
White	0.5	—	52.0	16.4	16.0	1.2	—	13.9
Black	1.3	62.0	5.8	3.3	12.6	1.3	8.7	5.0
Light-grey	11.6	0.4	8.4	9.5	69.0	—	—	1.1
Dark-grey	20.6	—	6.3	6.7	64.0	0.9	—	1.5
<u>UBC</u> area	12.9	—	18.9	10.6	53.0	0.6	—	4.0
White	1.7	—	46.0	15.1	17.3	1.5	—	18.4
Black	42.0	—	8.2	4.7	33.0	—	7.9	4.2
Light-gray	4.8	—	27.0	15.5	51.0	—	—	1.7
Dark-gray	20.1	—	6.5	6.7	64.0	0.9	—	1.8

LBC = lower bond coat, UBC = upper bond coat.

The light-grey phase has a higher chromium and cobalt content, and less aluminium and nickel, than the light-grey phase in the lower bond coat. The composition of the dark-grey phase is practically the same as that in the lower bond coat. The principal difference between the lower and upper bond coat is the presence of titanium in the former, this element being absent in the latter.

Fig. 2 shows the effect of time on the microstructural changes within the heat shield. The alumina layer separating the upper bond coat and the thermal barrier coating has grown to $\sim 30 \mu\text{m}$ in thickness after 300 hours and $\sim 50 \mu\text{m}$ after 600 hours. At some time between 600 and 900 hours, the thermal barrier coating became detached. No change in the bulk chemical analyses of the base metal and thermal barrier coating was detected, even after 2000 hours. A diffusion front, moving from the interface with the base metal up through the lower bond coat at a rate of approximately 0.1 μm per hour, was observed. Fig. 2 shows the changes in structure to the upper and lower bond coats. From “as received” (Fig. 1b) through 300 hours to 600 hours, there is a coarsening of the phases present. By 900 hours, after the loss of the thermal barrier coating, there are only two major phases present, light-grey and dark-grey. The white-coloured phase has disappeared completely, the elements having diffused into the light-grey coloured phase. As heat treatment time increased, the light-grey phase became the most dominant, and by 2000 hours, the dark-grey phase was quite depleted. The black phase in the lower bond coat, rich in titanium and nitrogen, coarsened. The coarsening of this phase, most likely to be TiN_{1-x} , may be a result of nitrogen from the furnace atmosphere diffusing into the bond coat directly at the cut sides of the samples, and may not be expected to occur so rapidly, if at all, in larger specimens. Nitrogen may also have entered the bond coat with the plasma spray if the coating powders had been stored under nitrogen.

An X-ray diffraction pattern of the top surface (upper bond coat with some retained alumina), Fig. 3, shows that the dominant light-grey phase is Ni_3Al , the γ' phase. The depletion of aluminium in the damage and repair cycle of the bond coat protective scale affects the diffusion mode and composition of the bond coat phases such that, below a critical aluminium concentration, the nickel-rich phases tend to form γ' Ni_3Al , the growth of which signifies the onset of rapid oxidation.

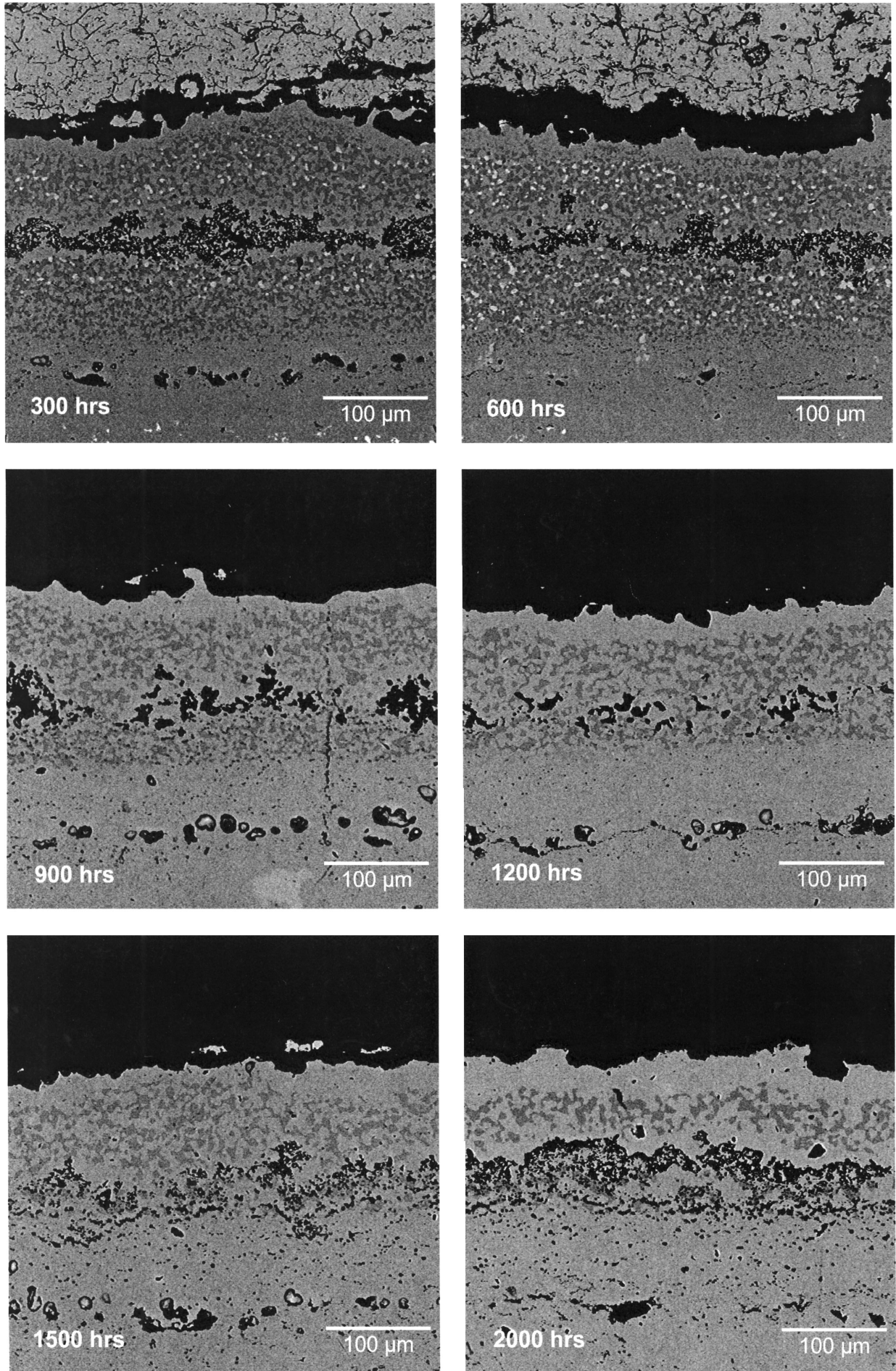


Figure 2 Changes in microstructure of the bond coat region in the heat treated samples. After 600 hours heat treatment at 1075°C, the thermal barrier coating has become detached.

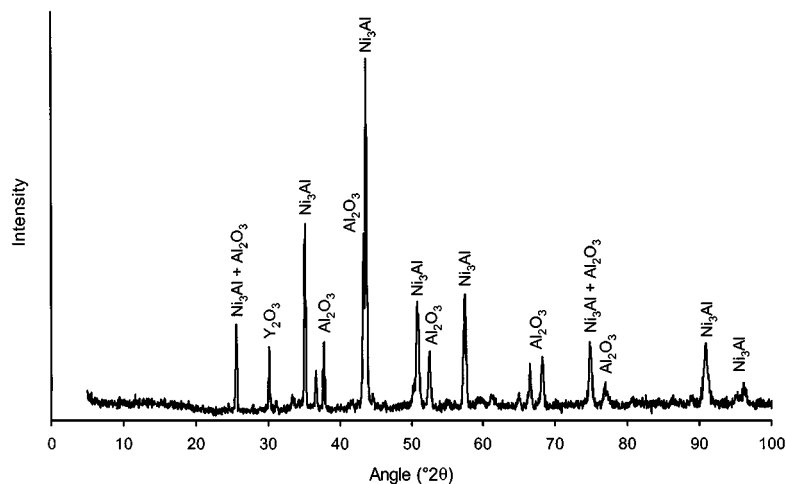


Figure 3 X-ray diffraction pattern of the top surface, the upper bond coat with part of the alumina layer from the sample, after 2000 hours heat treatment. The dominant phase, light-grey, is the γ' phase, Ni_3Al . The strongest yttria peak (at $2\theta = 30^\circ$) is also present.

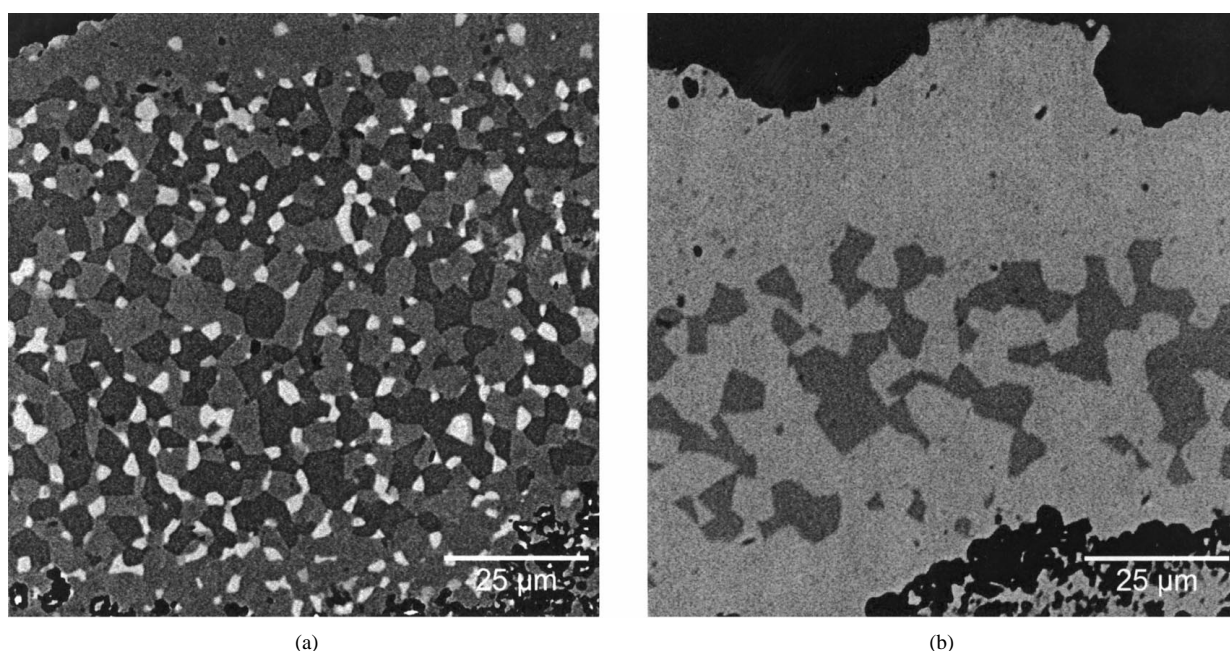


Figure 4 A detailed comparison between the upper bond coat in (a) the “as received” condition, and (b) the sample after 2000 hours at 1075°C.

The γ' phase penetrates the coating and causes rapid failure [11].

The compositions of the phases present after 2000 hours treatment are shown in Table IV. Almost all of the yttrium has diffused from the two bond coats to the upper-lower bond coat interface, as discussed below. A detailed comparison between the upper bond coat in the “as received” and 2000 hour samples is shown in Fig. 4.

The distribution of elements through the sample was studied by taking spot chemical analyses at equally spaced intervals along a linescan. Fig. 5 shows a line of 200 points over 300 μm in the 1500 hour sample. The results of the linescan are shown in Fig. 6. Fig. 6a displays the aluminium, oxygen and yttrium data. The position of the alumina layers, at 0–10 μm and 120–140 μm , is apparent. The yttrium that was present in the bond coats has migrated to the interface. This is

TABLE IV Chemical analyses (in wt%) of the phases present in the lower and upper bond coat after 2000 hours at 1075°C

Phases	Al	Ti	Cr	Co	Ni	Y	N	Others ^a
LBC area	6.4	13.3	16.8	10.2	44.0	—	3.6	5.7
Black	0.4	77.0	1.5	0.9	3.6	—	6.8	9.8
Light-grey	5.7	0.4	23.3	13.4	51.0	—	—	6.2
Dark-grey	18.2	0.3	8.0	8.0	64.0	—	—	1.5
UBC area	11.8	—	16.3	10.5	58.0	0.5	—	2.9
Light-gray	6.9	—	22.4	13.0	52.0	—	—	5.7
Dark-gray	18.4	—	7.9	7.3	65.2	—	—	1.2

^aThe other elements present have been withheld for commercial reasons.

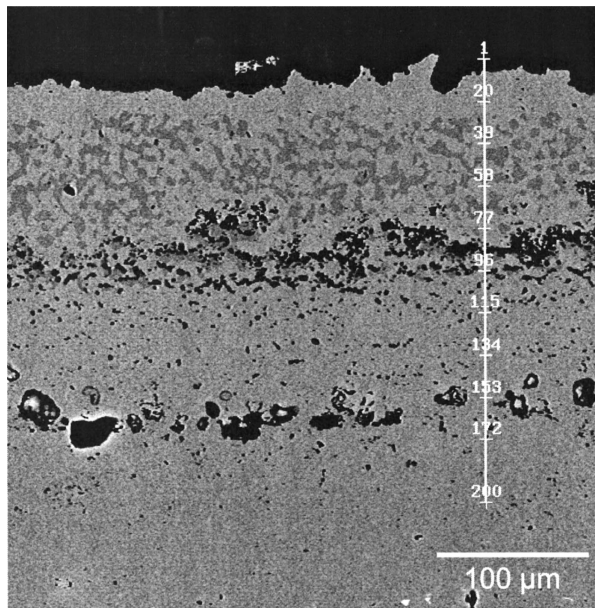
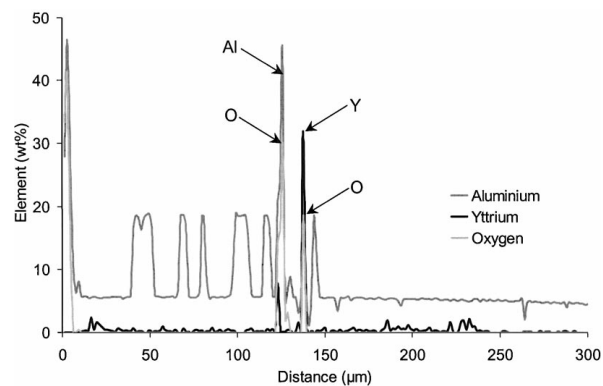


Figure 5 Micrograph of the sample after 1500 hours heat treatment, showing the position of the linescan (200 points over 300 μm) from the top of the upper bond coat through to the base metal.

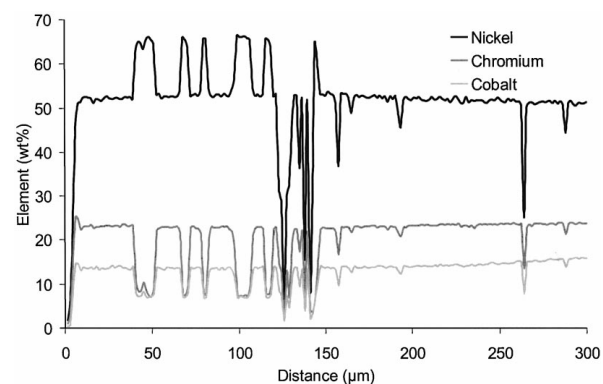
evident in the XRD pattern from the top surface protective alumina scale, Fig. 3, which shows the strongest yttria peak. Yttrium has been demonstrated to improve the adherence of protective alumina scales [1, 5, 9, 12]. Several possible mechanisms have been suggested [12]: (a) that yttrium could be oxidised into “pegs” within the alumina scale which improves its mechanical adherence to the bond coating; (b) small concentrations of yttrium in solid solution in the scale may reduce the growth rate; and (c) segregation of yttrium to the scale grain boundaries may also reduce growth rates and improve adhesion at elevated temperatures.

Fig. 6b displays the linescan data for nickel, chromium and cobalt. Along with the data for aluminium in Fig. 6a the differences in composition between the light-grey and dark-grey phases are quite distinct. The reduction in nickel, chromium and cobalt at the bond coat-bond coat interface is also apparent. Fig. 6c and d demonstrate that zirconium, niobium and tantalum only occur in the titanium-rich phase, and this is present primarily at the bond coat-bond coat interface and the interface between the lower bond coat and the base metal (at 260 μm). These elements do not, however, occur in the alumina phase itself.

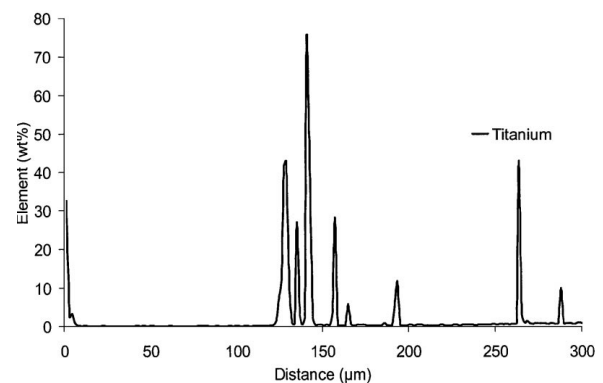
Further changes in composition within the sample due to diffusion have been observed with time. Linescans were performed from the lower bond coat into the base metal, again 200 points over 300 μm , to determine the extent of any diffusion (Fig. 7). The results for aluminium, titanium, nickel, cobalt and tungsten are displayed in Fig. 8. Both aluminium and titanium (Fig. 8a) can be seen to have diffused over a region of ~ 250 μm , both having a uniform gradient with a range of 2 wt%. Fig. 8b shows nickel diffusing over the same distance, from just under 53 wt% in the lower bond coat to 49 wt% in the base metal. Cobalt increases from ~ 14 wt% in the lower bond coat with a uniform concentration gradient over 250 μm to almost 19 wt%,



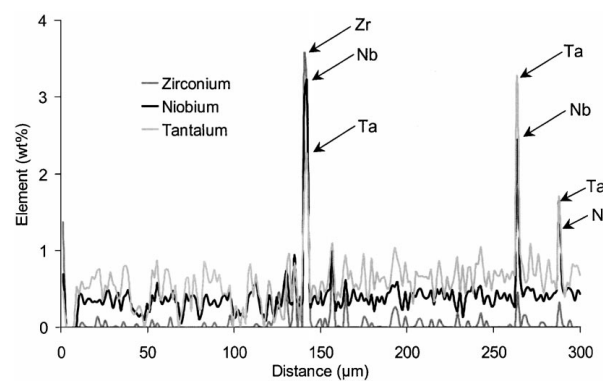
(a)



(b)



(c)



(d)

Figure 6 Linescan results for the 1500 hours sample in Fig. 5, showing the distribution of (a) aluminium, oxygen and yttrium, (b) nickel, chromium and cobalt, (c) titanium, and (d) zirconium, niobium and tantalum.

Fig. 8c. Tungsten, Fig. 8(d) increased over a slightly smaller distance, ~ 200 μm , from 1 wt% to 3 wt% in the base metal. Although the concentration of some elements present in the coating phases are small, they

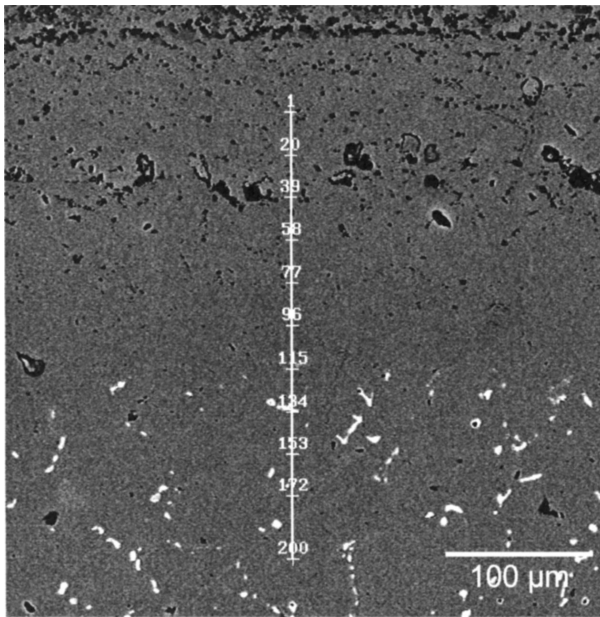


Figure 7 Micrograph of the sample after 1500 hours heat treatment, showing the position of the linescan (200 points over 300 μm) from the lower bond coat into the base metal.

do play an important role. For example, tantalum and tungsten are refractory metals which increase stability against diffusion; tantalum also enhances resistance to hot corrosion [5].

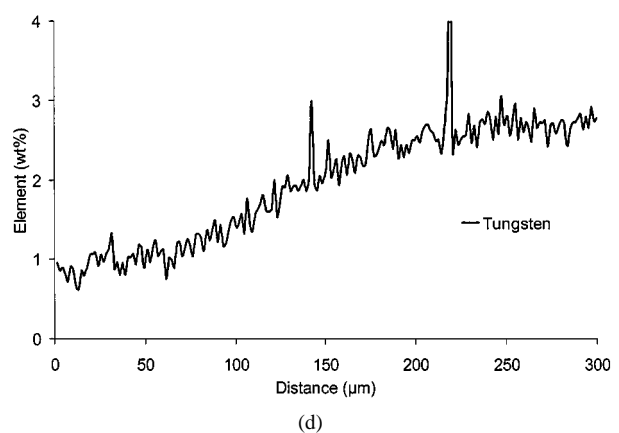
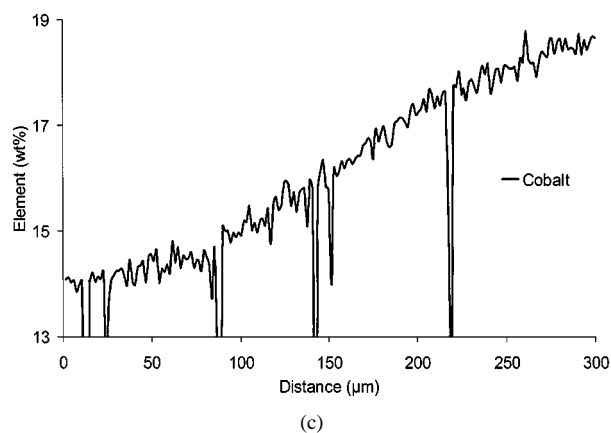
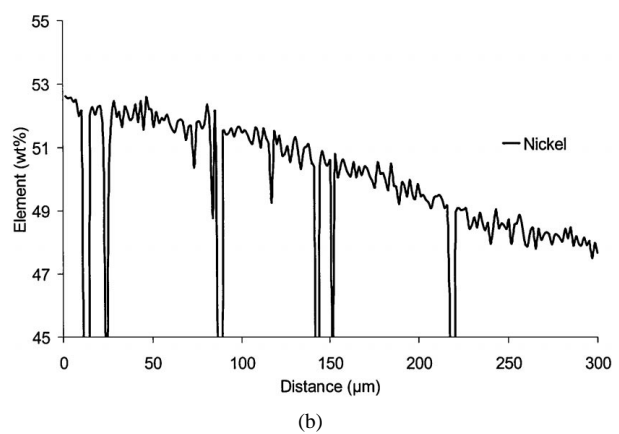
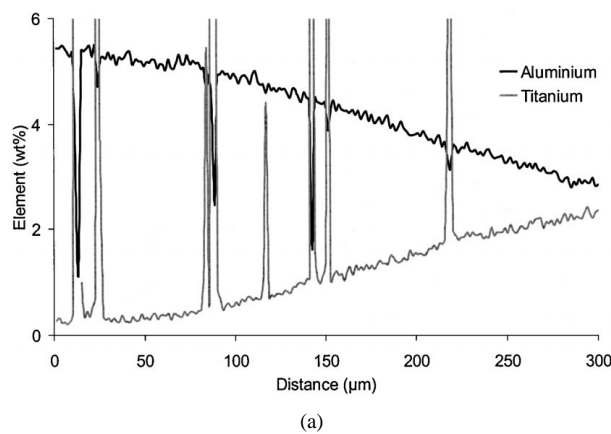


Figure 8 Linescan results for the 1500 hours sample in Fig. 7, showing the diffusion profiles for (a) aluminium and titanium, (b) nickel, (c) cobalt, and (d) tungsten.

4. Conclusions

Coated samples taken from a gas turbine combustion chamber heat shield have been exposed to an air atmosphere at 1075°C for up to 2000 hours.

(1) The alumina layer on the bond coat, adjacent to the thermal barrier coating, grew to a thickness of $\sim 50 \mu\text{m}$ after 600 hours heat treatment.

(2) The thermal barrier coating separated from the bond coat at some time between 600 and 900 hours heat treatment.

(3) The composition of the thermal barrier coating and the bulk base superalloy remained unchanged throughout the heat treatment programme.

(4) The principal phase in the bond coat was identified as the γ' phase, Ni_3Al . This phase grew to become dominant after 2000 hours of heat treatment.

(5) The alumina scale and the alumina phase at the bond coat-bond coat interface were the only yttrium-containing phases after 900 hours heat treatment.

(6) The elements present in the white-coloured phase in the “as received” sample were redistributed to the light-grey γ' phase over time.

(7) A TiN_{1-x} phase was present in the lower bond coat; this phase coarsened with time. This was the only phase found to contain zirconium, niobium and tantalum after 1500 hours or more, primarily near the upper-lower bond coat interface.

(8) Extensive diffusion of aluminium, titanium and nickel from the bond coat, and cobalt, tantalum and

tungsten to the bond coat was observed in samples given the longer heat treatments.

Acknowledgements

The authors gratefully acknowledge the following members of the Department of Materials at Imperial College: Mr B H Yoon for sample preparation; Mr M Haddon for XRD analysis; Dr L Christodoulou and Mr J Vyas for technical advice.

References

1. J. R. NICHOLLS and D. J. STEPHENSON, *High temperature coatings for gas turbines*, in "Intermetallic Compounds Principles and Practice," Vol. 2, edited by J. H. Westbrook and R. L. Fleischer (John Wiley and Sons, 1995) p. 489.
2. J. E. RESTALL, *Metallurgia* **46** (1979) 676.
3. F. S. PETTIT and G. W. GOWARD, *Gas turbine applications*, in "Coatings for high temperature applications," edited by E. Lang (Applied Science Publishers, 1983) p. 341.
4. A. BENNETT, *Materials Science and Technology* **2** (1986) 257.
5. G. W. GOWARD, *ibid.* **2** (1986) 194.
6. N. CZECH, F. SCHMITZ and W. STAMM, *Surface and Coatings Technology* **68/69** (1994) 17.
7. J. T. DEMASI-MARCIN and D. K. GUPTA, *ibid.* **68/69** (1994) 1.
8. R. SIVAKUMAR and B. L. MORDIKE, *ibid.* **37** (1989) 139.
9. J. R. NICHOLLS, K. J. LAWSON, L. H. AL YASIRI and P. HANCOCK, *Corrosion Science* **35** (1993) 1209.
10. R. L. APPS, *Journal of Vacuum Science and Technology* **11** (1974) 741.
11. M. G. HOCKING, V. VASANTASREE and P. S. SIDKY, "Metallic and ceramic coatings" (Longman Scientific and Technical, 1989).
12. H. M. TAWANCY, N. M. ABBAS and A. BENNETT, *Surface and Coatings Technology* **68/69** (1994) 10.

*Received 24 August
and accepted 26 October 1999*